PERGAMON

International Journal of Multiphase Flow 26 (2000) 229–244

International Journal of Multiphase Flow

www.elsevier.com/locate/ijmulflow

An experimental study of the effect of gas density on the distortion and breakup mechanism of drops in high speed gas stream

C.H. Lee, Rolf D. Reitz*

Engine Research Center, University of Wisconsin, Madison, Madison, WI 53706, USA

Received 6 May 1998; received in revised form 16 March 1999

Abstract

High velocity, gas-assisted liquid drop atomization processes were investigated under well-controlled experimental conditions at elevated gas densities and room temperature. A monodisperse stream of drops which are generated by a vibrating-orifice drop generator was injected into a transverse high velocity gas stream. The gas density and air jet velocity were adjusted independently to keep the Weber numbers constant. The Weber numbers studied were 72, 148, 270, and 532. The range of experimental conditions studied included the three drop breakup regimes previously referred to as bag, stretching/thinning and catastrophic breakup regimes. High-magnification photography was taken to study the microscopic breakup mechanisms in high velocity gas flow fields. When the Weber number is held constant at different gas densities and jet velocities, the results show that the microscopic breakup process is similar, even at high gas densities. At low Weber numbers, the photographs confirmed the existence of the bag breakup regime. The stretching/thinning breakup regime was observed for Weber numbers between 150 and 270. At Weber number = 532, the breakup in the catastrophic breakup regime occurred.

Keywords: Liquid drop; Drop distortion; Drop breakup; Gas density

1. Introduction

Power generating machines such as diesel and gasoline engines, gas turbines and rocket engines operate by burning liquid fuel. The combustion efficiency and pollutant emissions from

* Corresponding author.

0301-9322/00/$ - see front matter
PII: S0301-9322(99)00020-8

these engines are dependent on the rate of drop vaporization, the fuel/air mixing rate and the spatial distribution of the liquid drops. The liquid fuel atomization process has a strong influence on vaporization rates because the total surface area of the fuel is increased greatly by the atomization process. Understanding the mechanisms of the liquid drop atomization process is important in developing high efficiency engines.

Atomization can be enhanced by increasing the relative velocity between the liquid fuel and the ambient gas, as described by Chigier and Reitz (1996), Lefebvre (1989), and Hwang et al. (1996). The fundamental mechanisms of atomization have been under extensive experimental and theoretical study for many years. Reviews of liquid atomization mechanisms have been provided by Reitz and Bracco (1986), Krzeczkowski (1980), Pilch and Erdman (1987), Hsiang and Faeth (1992), Wu and Faeth (1993), and Gelfand (1996).

Studies of single liquid drop breakup mechanisms are of interest since they form the foundation of the study of atomization. At high relative velocity between the drops and gas the physical mechanisms of atomization are still poorly understood. As the relative velocity between a drop and the surrounding gas is increased, three basic breakup regimes are encountered which have been referred to as the bag breakup regime (Kenndy and Roberts, 1990), the 'shear' or 'boundary layer stripping' breakup regime (Ranger and Nicholls, 1969), and the catastrophic breakup regime (Reinecke and Waldman, 1970). The high-velocity drop breakup mechanism has been studied by Liu and Reitz (1997) who have pointed out that the widely referred to shear or boundary layer stripping mechanisms are not consistent with their experimental results. Instead, the breakup mechanism in that regime originates from drop flattening by aerodynamic effects. They suggest that this regime be referred to as a stretching or thinning breakup regime instead of a 'boundary-layer stripping' regime.

Some criteria for predicting drop breakup regime transitions in steady high speed gas flows have been presented by Krzeczkowski (1980), Wu et al. (1993) and other researchers. The Weber number, $We = \rho_G U^2 d/\sigma_L$ (where ρ_G is the gas density, U is the relative velocity between the drop and the gas, d is the drop diameter and ρ_L is the surface tension of the liquid), and the Ohnesorge number, $Z = \mu_L/(\rho_L d\sigma)^{1/2}$ (where μ_L is the liquid viscosity, ρ_L is the liquid density) have been found to be important parameters. For Ohnesorge numbers less than one ($Z < 1$, i.e., all but the most viscous fluids) significant drop distortion and oscillation is noticed starting at $We \sim 1$ (the Weber number is based on the undistorted drop diameter). The bag breakup regime begins at $We = 12$. Transition to the so-called 'shear-type' breakup occurs at higher Weber numbers ($We > 80$) and 'multimode' breakup (combined bag and thinning (shear)) occurs in the intermediate Weber number range (Wu et al., 1993). For high viscosity liquids, Wierzba and Takayama (1988) and Wu et al. (1993) concluded that the Ohnesorge number must be introduced and the breakup regime transitions are moved to higher Weber numbers.

The breakup of high velocity drops at high ambient gas densities is of much interest in many practical applications. As the drop velocity and air density increase, aerodynamic and possibly viscous effects are expected to become more important and the breakup process becomes more complex. In combustion engine applications, the fuel is injected into high density air which has been compressed during the compression stroke in an IC engine or by a compressor in a gas turbine. A detailed insight into the fundamental mechanisms which control the breakup of high speed liquid drops in a high density gas has not been investigated previously and thus models

of disintegration are still only speculative and based on tests performed under atmospheric conditions (e.g. Hwang et al., 1996; Wu et al., 1993).

Most fundamental drop breakup research has been performed under atmospheric condition due to the experimental difficulties encountered in tests at elevated pressures. An investigation on the effect of gas density on drop breakup was performed in a shock tube by Gelfand et al. (1975) and Gelfand (1996) who investigated drop breakup with changing initial pressures. The drop breakup mechanism at high initial gas pressure ($P_0 = 3$ MPa) was found to resemble that of atmospheric pressure ($P_0 = 0.1$ MPa). It was also found that the breakup process required less time at a raised gas pressure.

The objective of the present work was to investigate gas density and velocity effects on the breakup mechanisms of liquid drops injected into a transverse high velocity gas flow at various back pressures, i.e., by varying the gas density and gas velocity in a spray chamber. The experiments were performed for four Weber number cases (72, 148, 270, 532) and four spray chamber pressures (1, 3.7, 6.4, and 9.2 atm). The breakup regimes with Weber numbers 72, 148–270, 532 represent breakup in the bag, stretching/thinning and catastrophic breakup regimes, respectively. Based on the information presented by the experimental results, the breakup mechanisms of liquid drops in the three breakup regimes were analyzed.

2. Experimental apparatus

The liquid drop generator and gas nozzle with a converging exit were arranged in a cross-

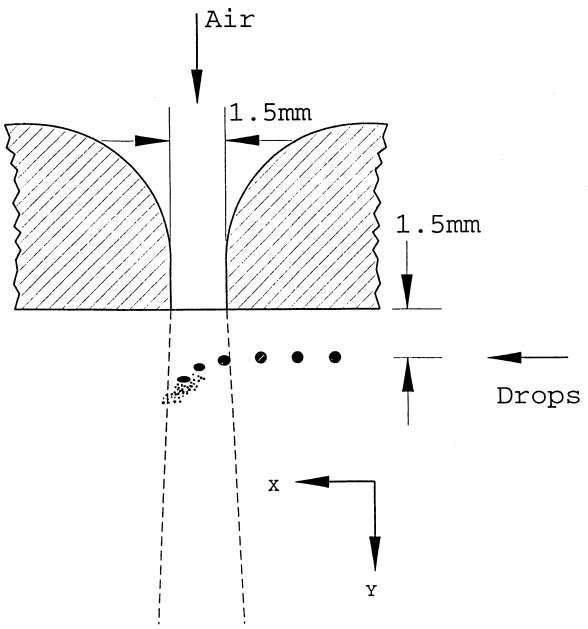

Fig. 1. Schematic diagram showing drop breakup with the transverse gas jet.

flow pattern as shown in Fig. 1. The experimental apparatus consisted of a high pressure spray chamber, liquid drop generator, gas nozzle, light source, long-distance microscope, and camera as shown in Fig. 2. The gas nozzle was circular in shape with a diameter of 1.5 mm. The 5 mm-long-air nozzle passage featured a rounded entrance with curvature radius $R = 5$ mm, to ensure that the velocity profile at the nozzle exit was flat so that boundary-layer effects at the nozzle exit could be minimized. This ensured that the drops entering the gas stream were suddenly exposed to a high relative velocity. The air flow rate was monitored by a rotameter. In order to maintain a constant differential pressure between the fuel injection pressure and the spray chamber back pressure, a combination of check valves and a purge valve was properly used, as shown in Fig. 2.

The monodisperse droplet stream was generated using a Berglund–Liu vibrating-orifice drop generator (Berglund and Liu, 1973). The drop size generated was determined from the relationship $d = (6Q/\pi f)^{1/3}$, where Q is volumetric flow rate and f is the applied frequency. The optimum frequency was obtained from the Rayleigh wavelength for the most unstable disturbance, viz., $f_{\text{Rayeigh}} = V_j/\lambda_{\text{optimum}} = 0.282Q/D_j^3$, where D_j is the injector orifice diameter, V_j is the liquid jet velocity, and λ_{optimum} is the wavelength of the most unstable disturbance. In this study, a 100 μm diameter orifice was used. The generated drop size was constant at 184 μm and f was 30 kHz. The piezoelectric drop generator was operated using a square-wave signal with peak-to-peak voltage 20 V. The differential pressure between the fuel injection pressure and the spray chamber back pressure was maintained at 275 kPa, and under these conditions each drop was ejected at an average velocity of 18 m/s, as determined from measuring the

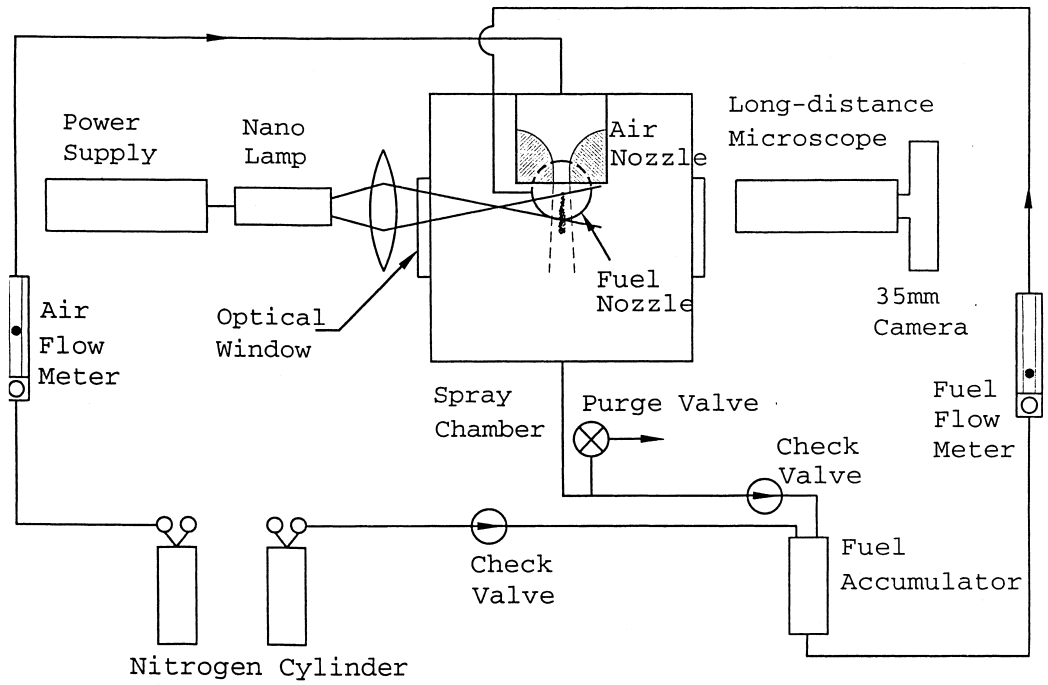

Fig. 2. Schematic diagram of the optical arrangement.

volume flow rate. The fuel flow rate was monitored by a rotameter and controlled with a precision control valve.

The fuel used was Benz oil UCF-1 test fuel, which meets SAE J967d, ISO 4113 (a diesel-type fuel). The technical specifications of the fuel were: viscosity 0.00217 Ns/m^2, density 840 kg/m^3, surface tension 0.02 kg/s^2, flash point 348 K, and t-90 distillation point 483 K.

The microscopic spray visualization system consisted of a Xenon high-intensity nanopulse light source and a 35 mm camera equipped with a Questar QM-100 long-distance microscope lens. The pulse duration was 20 ns. High-sensitivity T-Max 400 or 3200 film was used for the photography. The magnification was $\times 15$ on the film negatives. Considerations of the diffraction limits of the lens system used led to the estimate that dimensions can be resolved in the photographs down to 3 μm (Liu and Reitz, 1993).

The experiments were performed for the 16 cases shown in Table 1, which were four Weber number cases (72, 148, 270, 532) at four spray chamber pressure (1.0, 3.7, 6.4, and 9.2 atm). The jet gas was nitrogen. Table 1 also includes the drop Reynolds number based on the gas properties, $Re_G = \rho_G U d/\mu_G$ and the Weber numbers.

3. Drop breakup theories

As the relative velocity between the drop and the ambient gas is increased, various drop breakup regimes are encountered. The regimes reflect qualitative differences in the drop

Table 1
Summary of the experimental conditions[a]

	Weber number, $We = \rho_G U^2 d/\sigma_L$	Spray chamber pressure, P_b (MPa)	Density of gas ρ_G (kg/m^3)	Velocity of gas jet, U (m/s)	Reynolds number $Re = \rho_G U d/\mu_G$
1	72	0.10	1.2	82	990
2	72	0.37	4.3	42	1889
3	72	0.64	7.5	32	2492
4	72	0.92 (0.85)	10.6 (9.8)	27 (28)	2991 (2871)
5	148	0.10	1.2	118	1425
6	148	0.37	4.3	61	2744
7	148	0.64	7.5	46	3582
8	148	0.92 (0.85)	10.6 (9.8)	39 (40)	4321 (4102)
9	270	0.10	1.2	159	1920
10	270	0.37	4.3	82	3688
11	270	0.64	7.5	62	4829
12	270	0.92 (0.85)	10.6 (9.8)	52 (54)	5761 (5538)
13	532	0.10	1.2	223	2693
14	532	0.37	4.3	115	5173
15	532	0.64	7.5	87	6776
16	532	0.92 (0.85)	10.6 (9.8)	73 (76)	8088 (7795)

[a] The experimental conditions in parentheses are for trajectory visualization conditions.

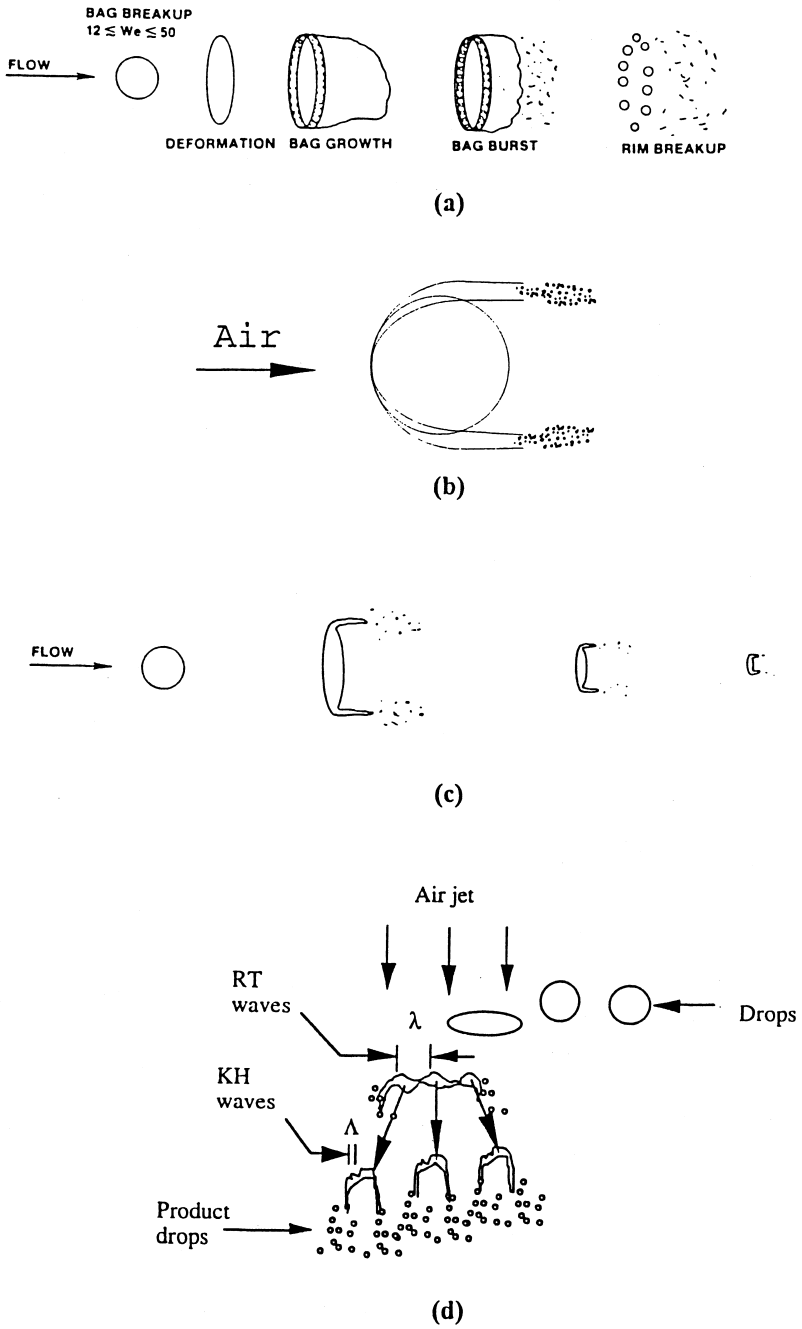

Fig. 3. Schematic diagram of breakup mechanisms, (a) bag breakup (Pilch and Erdman, 1987), (b) previously proposed shear or boundary layer breakup (Ranger and Nicholls, 1969), (c) alternative stretching/thinning breakup (sheet breakup) (Liu and Reitz, 1997) and (d) catastrophic breakup (Hwang et al., 1996).

breakup mechanism and yield different outcomes for the drop-breakup drop sizes. A brief review of previously proposed drop breakup mechanisms follows.

3.1. Bag-breakup mechanism

When drops are introduced into a low velocity air stream, the drops becomes flattened and a thin hollow bag is blown downstream which is attached to a more massive toroidal liquid rim. The bag eventually bursts, forming a large number of small fragments; the rim disintegrates after a short time later, producing a small number of large fragments (Pilch and Erdman, 1987; Wierzba, 1990). The typical bag breakup process is displayed in Fig. 3(a).

3.2. Shear or boundary layer stripping mechanism

As the relative velocity is increased, droplet breakup now originates from the equator of the drop. Early theories ascribed the breakup to a shear or 'boundary-layer stripping', as originally proposed by Ranger and Nicholls (1969), and Hinze (1955). A conceptualization of the hypothetical shear or boundary-layer stripping breakup process is shown in Fig. 3(b). In this model, viscous boundary layers develop in the drop and in the surrounding gas and the accelerated liquid is thought to be stripped from the drop at its equator (e.g., Collins and Charwat, 1971). Delplanque and Sirignano (1994) argue that the appropriate criterion for stripping is when surface tension no longer balances the centrifugal acceleration that a fluid particle in the liquid boundary layer undergoes. They assume that the mass removal rate of fluid leaving the droplet is equal to the mass flux of the liquid in the boundary layer at the equator.

Considerable work has been done by Anilkumar et al. (1993), Lee et al. (1993), and Danilov and Mironov (1992) dealing with the breakup of drops in high intensity sound fields. In these levitating drop experiments the drop is always fixed spatially during the flattening process, making the study of breakup easier. These works are of interest to the present study because the acoustic pressure is analogous to the dynamic pressure effect in steady flows, as concluded by Danilov and Mironov (1992). Under the action of an intense sound field the flattened drop also deforms into a knife-edged disc structure and breakup occurs at the thinned equatorial edge of the drop. This forms the basis of an alternative theory of high speed drop breakup which has been called stretching/thinning breakup by Liu and Reitz (1997).

3.3. Stretching/thinning breakup mechanism

When the air stream velocity is increased, due to the high velocity at the equator of drop, a suction stress toward the outside of the drop occurs in the horizontal direction, which leads to the horizontal extension of the drop. From mass conservation, the thickness of the flattened drop will decrease from its center to the edge, and ultimately the edge will be very thin, and thus tend to follow the air flow direction, due to its low inertia (Liu and Reitz, 1997). It appears that the very thin edge sheet of the flattened drop, which has a low inertia, is deflected in the direction of the gas flow by the blowing of the air stream (Fig. 3(c)). This causes the flattened drop to present a convex surface facing the air stream. The breakup of the deflected

sheet then evidently occurs by a mechanism which is similar to 'the stretched streamwise ligament breakup' mechanism described by Stapper and Samuelson (1990).

3.4. Catastrophic breakup mechanism

At sufficiently high air velocities, the drop experiences an even larger dynamic pressure change on its surface (Engel, 1958). A similar situation is found when a stationary drop is exposed to a shock wave or to a very high-intensity sound wave. Anilkumar et al. (1993) found that large-scale instability waves were generated on the flattened droplet surface under acoustical levitation. Similar waves have been identified by Hwang et al. (1996) for drops in a high velocity gas flow. Once again the drop is flattened into the form of a sheet and the accelerating sheet breaks into a large-scale fragments by means of Rayleigh–Taylor instability. Much shorter wavelength, Kelvin–Helmholtz waves, originate at the edges of the fragments and these waves are stretched to produce ligaments, which then break up into very small droplets. These processes are illustrated schematically in Fig. 3(d) (Hwang et al., 1996).

4. Results and discussion

The high speed gas jet and liquid fuel drops were injected to form a cross flow configuration as shown in Fig. 1. The optical system in Fig. 2 was used to take high magnification, ultra-short duration pulse-illumination photographs. The residence time (t_c) of the drop in this experiment as it passes the gas jet is approximately 25 μs. Hwang et al. (1996) found that considerable flattening of the drop is seen to have occurred in times order of 20–25 μs in the stripping/thinning breakup regime. They also found that considerable breakup of the drop occurs within 25 μs in the catastrophic breakup regime. Thus, a short residence time is sufficient for visualizing the whole process of the drop breakup. However, in the case of the bag breakup regime, the residence time in the field of view is not long enough for complete visualization of the breakup process and only the initial distortion and bag formation details are revealed. The analysis of the breakup mechanisms is based on qualitative observations of Figs. 4–7.

From the photographs, the breakup processes of drops injected into four different gas densities, i.e., four different spray chamber back pressures were investigated by changing the gas velocity, while the Weber number was maintained constant for a given gas density. From inspection of the photographs, it was found that the breakup processes show similar behavior at a fixed Weber number. Also, the breakup processes could be classified roughly into two stages, in agreement with the findings of Liu and Reitz (1997), who examined the effect of drop diameter on the breakup process. The present study focuses on the effect of the gas density.

4.1. Drop distortion and first breakup stage

When a spherical drop is introduced into a steady gas stream, the drop shape is influenced by the gas pressure distribution around the drop. Under equilibrium conditions the internal pressure at any point is just sufficient to balance the external aerodynamic pressure and the

surface tension pressure. However, when a steady air stream flows around a drop, the velocity distribution and the air pressure distribution at any point on the drop surface are not uniform. The air velocity is maximum at the equator of the drop, equals zero at the stagnation point at the drop's pole. Thus, in accordance with Bernoulli's law the air pressure is higher at the pole, and lower at the equator. This causes the drop to distort from its spherical shape and to become flattened to form an oblate ellipsoid, aligned normal to the air flow direction. The drop distortion process, at early times, is clearly seen in the present study as shown in

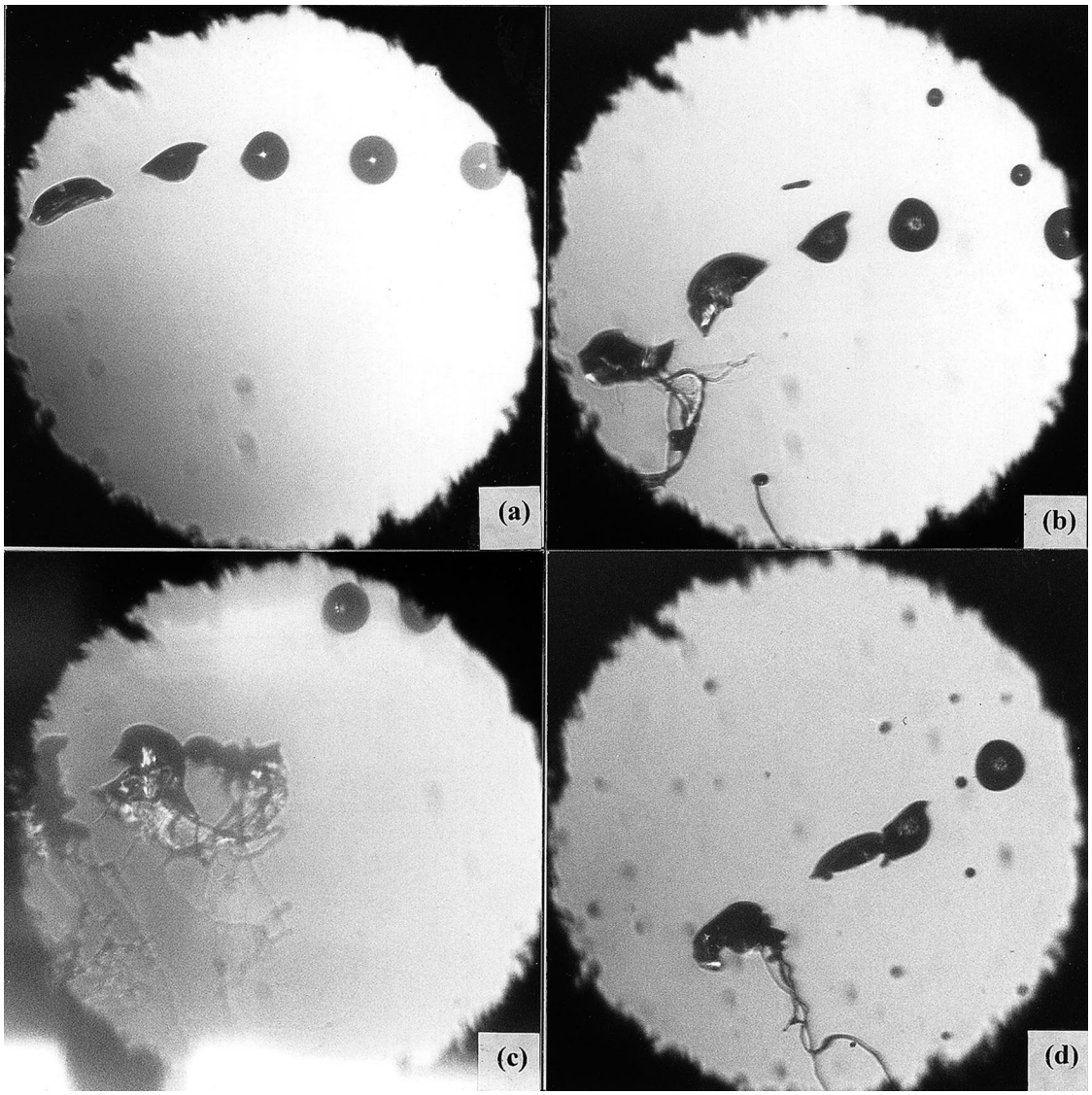

Fig. 4. Photographs of bag breakup of drops in gas jets whose density and velocity are, respectively (a) (1.2 kg/m^3, 82 m/s), (b) (4.3, 42), (c) (7.5, 32) and (d) (10.6, 27), respectively.

Figs. 4–7. In these figures the monodisperse train of drops enters at the top right of each frame and the air jet is oriented vertically downward.

4.2. Second breakup stage

As the relative velocity or the density of injected gas increases, the bag, so-called stretching/thinning and catastrophic breakup regimes are encountered, as shown in Figs. 4–7. The photographs show the drop breakup processes in the three regimes for 184 μm diameter

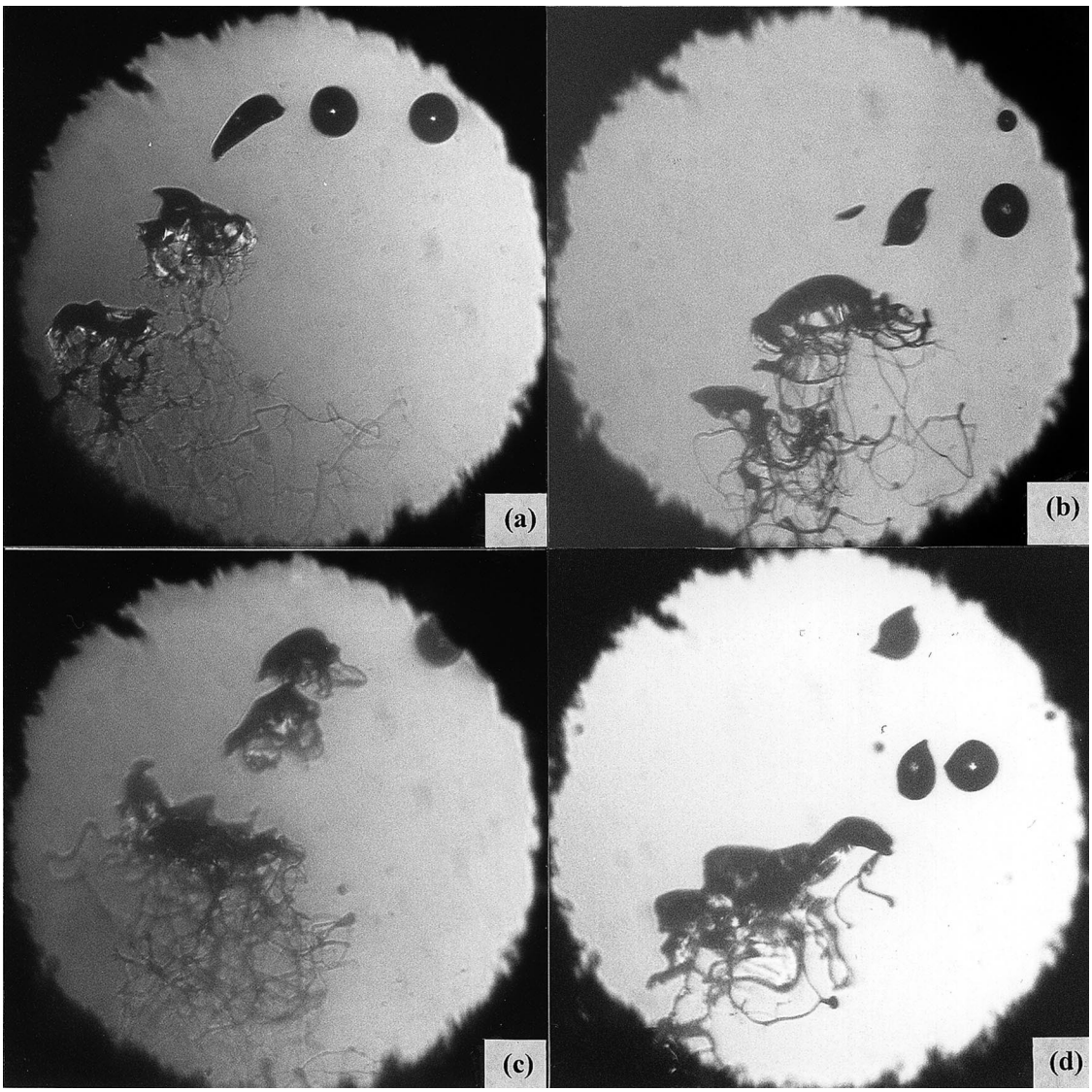

Fig. 5. Photographs of stretching breakup of drops in gas jets whose density and velocity are, respectively (a) (1.2 kg/m^3, 118 m/s), (b) (4.3, 61), (c) (7.5, 46) and (d) (10.6, 39), with a corresponding Weber number of 148.

injected drops. The Weber number was increased by increasing the velocity of injected gas velocity or the density of gas.

4.3. Bag breakup

When the air stream velocity is relatively low, the bag breakup phenomenon appears. The accelerating drop becomes increasingly flattened, and at a critical relative velocity, the flattened drop becomes thin enough that it presents a concave surface near its pole and soon it is blown

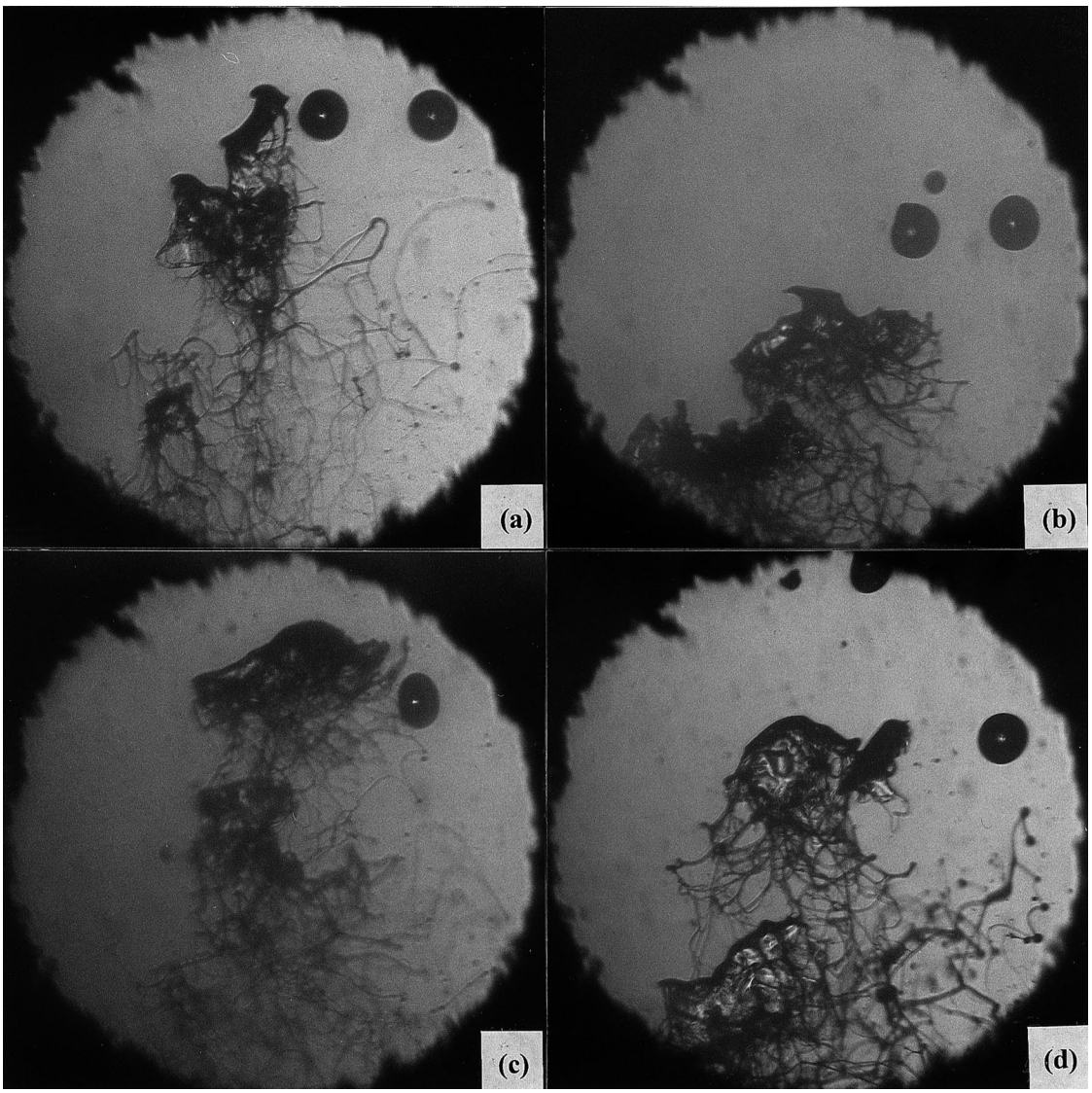

Fig. 6. Photographs of stretching breakup of drops in gas jets whose density and velocity are, respectively (a) (1.2 kg/m^3, 159 m/s), (b) (4.3, 82), (c) (7.5, 62) and (d) (10.6, 52), with a corresponding Weber number of 270.

out into the form of a thin hollow bag attached to a roughly circular rim. The bag is stretched and swept off in the downstream direction. The bag forms at the point where dynamic pressure is the highest, i.e, near the front stagnation point. The breakup and distortion of drops were investigated, in detail, by Liu and Reitz (1997) at atmospheric conditions. The present study includes the effect of elevated gas pressure (density).

Fig. 4 shows that bag breakup also occurs for liquid drops at elevated densities, which were 1.2 (case (a)), 4.3 (case (b)), 7.5 (case (c)), 10.6 (case (d)) kg/m^3, respectively. The corresponding gas stream velocities were 82 (case (a)), 42 (case (b)), 32 (case (c)) and 28 (case

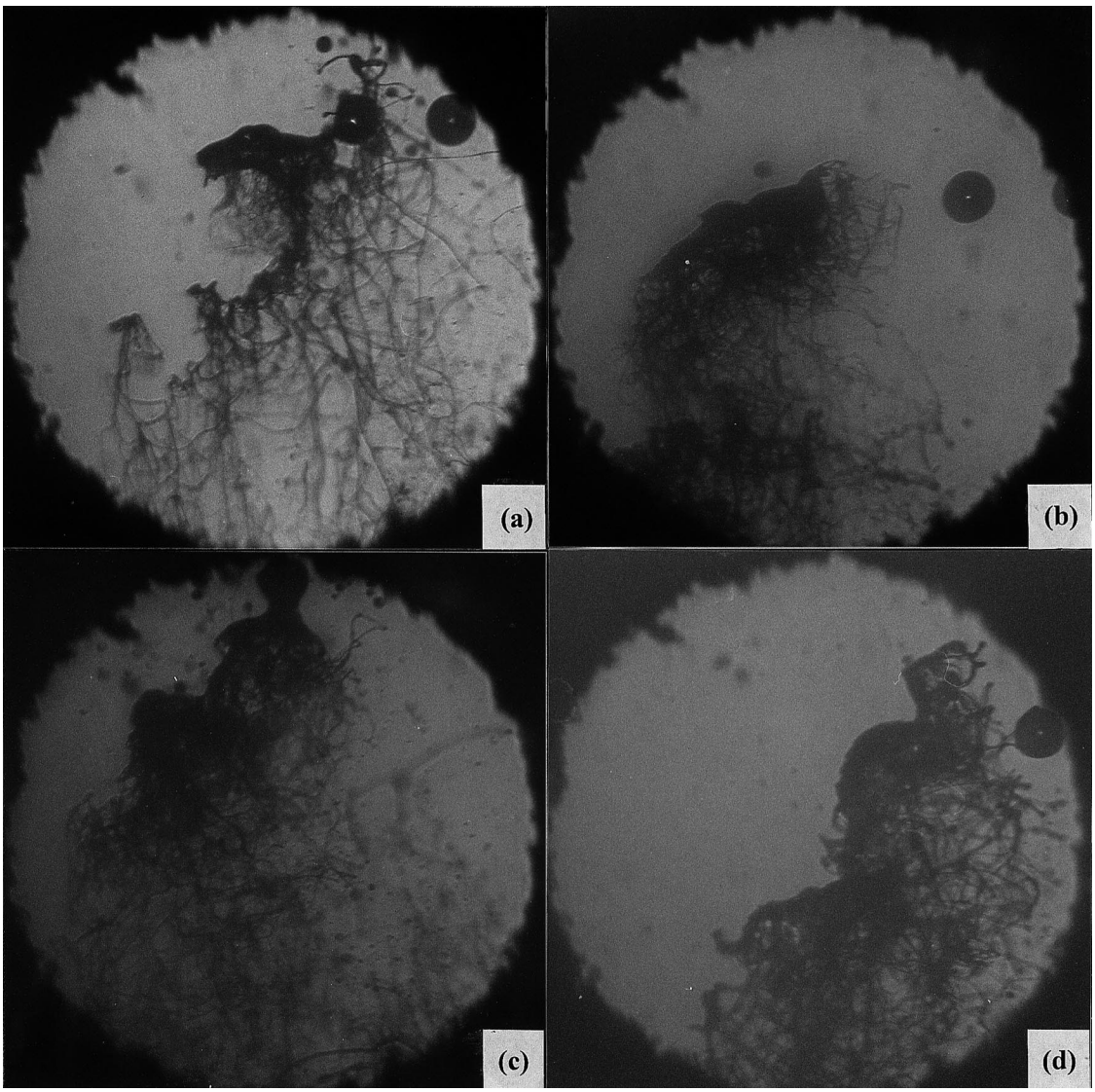

Fig. 7. Photographs of catastrophic breakup of drops in gas jets whose density and velocity are, respectively (a) (1.2 kg/m^3, 223 m/s), (b) (4.3, 115), (c) (7.5, 87) and (d) (10.6, 73), with a corresponding Weber number of 532.

(d)) m/s, respectively, in order to get a constant Weber number of 72 for four cases. The photographs show that the drop breakup process is similar at different gas density levels. In the case $\rho_G = 1.2$ kg/m^3, the drag force on the drops is the smallest of the four cases and the diameter of the gas nozzle is such that the drops' residence time in the uniform gas flow field is short enough that the drops move out of the other side of the gas jet before the bag is fully formed from the parent drops as shown in Fig. 4(a). The beginning of bags formed from the parent drop can be seen in Fig. 4(b)–(d). The deflection of the drops from their initially horizontal trajectory is increased with increasing gas density due to the higher drag force on the drops. This implies that the local drop-gas relative velocity changes during the interaction process differently when the gas density is changed. Nevertheless, the similarity of the breakup mechanism seen in the photographs at different gas densities indicates that the Weber number is the appropriate scaling parameter for drop breakup in the bag breakup regime.

4.4. Stretching/thinning breakup

As the gas velocity is increased further, breakup now occurs at the equatorial edges of the flattened drop, which can be seen in Fig. 5. The gas velocities and densities for cases (a), (b), (c) and (d) are (118 m/s, 1.2 kg/m^3), (61, 4.3), (46, 7.5) and (39, 10.6), respectively, with corresponding Weber number equal to 148. The breakup process is distinctly different from that in the bag breakup regime. Instead of its pole region being blown out into a thin hollow bag anchored to its rim (the equator), the drop is deformed in the opposite direction and it presents a convex surface to the flow of air. The edges of the saucer-shaped drop are drawn out into a thin sheet by drag forces, and then the sheet is split up into fine filaments or ligaments, which later break up into small drops. Because the velocity at the equator of the drop is high, a suction stress toward the outside of the drop occurs in the horizontal direction, which leads the observed horizontal extension of the drop. From mass conservation, the thickness of the flattened drop will decrease from its center to the edge, and the edge will be very thin. Thus, it tends to follow the air flow direction due to its low inertia (Liu and Reitz, 1997).

Similarly, in Fig. 6 ($We = 270$), for the different gas density conditions, the very thin edge sheet of the flattened drop is seen to be deflected in the direction of the gas flow around the drop. Stapper and Samuelson (1990) found that flat liquid sheets exposed to coflowing gases with high relative velocities exhibit cellular breakup patterns where thin liquid membranes are formed between growing streamwise waves. This led to the formation of streamwise ligaments which are also seen in the breakup of the sheet formed at the edges of the present drops.

As shown in Figs. 5 and 6, for four different gas densities, but constant Weber number, the breakup mechanism of the drops is similar. Once the ligaments are formed, their mechanism of breakup is likely to be similar to that of jet breakup; namely, Rayleigh capillary wave pinching which has been studied extensively both experimentally and theoretically (e.g., Reitz and Bracco, 1986).

In the boundary-layer-stripping model it is assumed that viscous shear forces in the air and liquid boundary layers are responsible for the liquid that is 'stripped from the drop's equator'. In the boundary-layer-stripping model it is presumed that viscous shear forces are dominant, and thus the breakup process should scale with the Reynolds number, since Reynolds number

is a ratio of inertia to viscous forces. However, as seen in Table 1, the present experimental results do not support this condition. In fact, it is obvious that the liquid breakup regimes scale instead with Weber number as shown in Figs. 4–7, and not with Reynolds number. For example, cases 3, 6 and 13 have similar Reynolds numbers (2492, 2744 and 2693, i.e., similar to within 10%) but, as seen in Figs. 4–7, they lie in completely different regimes (i.e., in the bag, so-called stretching/thinning and catastrophic regimes, respectively). On the other hand, the breakup regimes scaled well with Weber number, as shown in Table 1.

From the above analyses, it is concluded that the occurrence of drop breakup in this streching/thinning regime depends primarily on the value of the drop Weber number.

4.5. Catastrophic breakup

As the gas velocity or density is further increased, the so-called 'catastrophic' breakup phenomenon occurs. Fig. 7 shows a typical catastrophic breakup process of liquid drops which enter the nitrogen gas stream with four different densities, which are 1.2 (case (a)), 4.3 (case (b)), 7.5 (case (c)), 10.6 (case (d)) kg/m^3, respectively. The gas velocities were 223 (case (a)), 115 (case (b)), 87 (case (c)) and 73 m/s, respectively, in order to get a constant Weber number of 532 for all the cases. The photographs show that the drop breakup and distortion is similar if the Weber number is held constant while changing the gas density.

The similarities in the breakup phenomena in Figs. 6 and 7 for drops in the stretching and catastrophic breakup regimes suggests that they have analogous breakup mechanisms, i.e., (1) the sheet edge of the flattened drop is bent in the direction of flow of gas by the gas stream blowing, which makes the flattened drop exhibit a convex surface facing the gas flow, (2) production of folds on the thin edge sheet in the azimuthal direction caused by the bending of the sheet edge leads to the production of filaments (Liu and Reitz, 1997).

However, close examination of the flattened droplet surface reveals the existence of large wavelength surface waves (see Fig. 3(d)), as would be expected from the Rayleigh–Taylor instability of highly accelerated liquid drops in the catastrophic breakup regime (Hwang et al., 1996). In comparing Fig. 7(a) and (d), the ligaments of case (a) are stretched longer than those of cases (b), (c) and (d), due to the higher velocity of the gas jet and this results in the observed wider spatial distribution of ligaments which are stripped from the original drops.

In summary, the experimental results shown in Figs. 4–7 confirm that the drop breakup mechanisms depend primarily on the value of the Weber number in all three regimes for changing gas density and the gas jet velocity. A similar conclusion was reached by Liu and Reitz (1997) who varied the initial drop diameter and gas jet velocity. As summarized in Table 1, the drop breakup process does not scale with the Reynolds number, as would be expected if viscous or boundary layer effects were to be influential in the breakup process, as has been presumed in previous boundary-layer models.

5. Conclusions

The breakup and distortion of drops were investigated, in detail, by Liu and Reitz (1997) at atmospheric conditions. The present study includes the effect of elevated gas pressure (density),

and thus allows the dominant scaling effect of the Weber number in the breakup mechanism to be confirmed.

The present experimental studies have been performed by injecting liquid drops into a high-speed transverse gas jet to investigate the distortion and breakup mechanisms of the drops. The velocities and densities of the gas were changed to achieve independent control of the drop Weber number. Based on the experimental results and qualitative analyses of the photographs, it is found that the drop-breakup mechanism depends on the value of the Weber number in each breakup regime. Three breakup regimes, i.e., bag breakup, stretching/thinning breakup and catastrophic breakup appear as the Weber number is increased. The experimental results under varying gas density and velocity conditions confirm that the breakup in all three breakup regimes does not depend on the Reynolds number, as would be the case if viscous effects controlled the breakup process. This result confirms that of an earlier study (Liu and Reitz, 1997) and casts more doubt on the validity of previous shear or boundary-layer stripping drop breakup theories.

Acknowledgements

This work was supported by Army Research Office and Caterpillar. C. H Lee was supported by the Korea Science and Engineering Foundation. The authors thank P. Tennison, K. Tanin, Dr. H. Snyder and K. Richards for help in this research.

References

Anilkumar, A.V., Lee, C.P., Wang, T.G., 1993. Stability of an acoustically levitate and flattened drop: an experimental study. Physics of Fluids A 5, 2763–2774.

Berglund, R.N., Liu, Y.H., 1973. Generation of monodisperse aerosol standards. Exp. Sci. Technol. 7, 147–153.

Chigier, N.A., Reitz, R.D., 1996. Regimes of jet breakup of and breakup mechanisms. In: Kuo, K.(Ed.), Progress in Astronautics and Aeronautics, American Institute of Aeronautics and Astronautics, Reston, VA, vol. 1, pp. 109–136.

Collins, R., Charwat, A.F., 1971. The deformation and mass loss of liquid drops in a high speed flow of gas. Israel J. Tech 9, 43–54.

Danilov, S.D., Mironov, M.A., 1992. Breakup of a droplet in a high-intensity sound field. J. Acoust. Soc. Am. 92, 2747–2755.

Delplanque, J.-P., Sirignano, W.A., 1994. Boundary layer stripping effects on droplet transcritical convective vaporization. Atomization and Sprays 4, 325–350.

Engel, O.G., 1958. Fragmentation of water drops in the zone behind an air shock. Journal of Research National Bureau of Standards 60, 2747–2755.

Gelfand, B.E., Gubin, S.A., Kogarko, S.M., Palamarchuk, B.I., 1975. Sov. J. Appl. Mech. i Tech. Phys. 4, 61.

Gelfand, B.E., 1996. Droplet breakup phenomena in flows with velocity lag. Prog. Energy Combust. Sci. 27, 201–265.

Hinze, J.O., 1955. Fundamental of the hydrodynamic mechanism of splitting in dispersion process. AICHE J. 1, 289–295.

Hsiang, L.P., Faeth, G.M., 1992. Near limit drop deformation and secondary breakup. Int. J. Multiphase Flow 19, 635–652.

Hwang, S., Liu, S., Reitz, R.D., 1996. Breakup mechanisms and drag coefficients of high speed vaporizing drops. Atomization and Sprays 6, 353–376.

Kenndy, J.B., Roberts, J., 1990. Rain ingestion in a gas turbine engine. In: Proceedings of 4th ILASS Meeting, Hartford, CT, 154.

Krzeczkowski, S.A., 1980. Measurement of liquid droplet disintegration mechanism. Int. J. Multiphase Flow 6, 227–239.

Lee, C.P., Anilkumar, A.V., Wang, T.G., 1993. Static shape and instability of an acoustically levitate and flattened drop. Physics of Fluids A 3, 2497–2515.

Lefebvre, A.H., 1989. Atomization and Sprays. Hemisphere, New York.

Liu, A.B., Reitz, R.D., 1993. Effects of drop drag and breakup on fuel sprays. Atomization and Sprays 3, 55–75.

Liu, Z., Reitz, R.D., 1997. An analysis of the distortion and breakup mechanisms of high speed liquid drops. Int. J. Multiphase Flow 23, 631–650.

Pilch, M., Erdman, C.A., 1987. Use of breakup time data and velocity history data to predict the maximum size of stable fragments for acceleration-induced breakup of liquid drop. Int. J. Multiphase Flow 13, 741–757.

Ranger, A.A., Nicholls, J.A., 1969. The aerodynamic shattering of liquid drops. AIAA J. 7, 285–290.

Reinecke, W.G., Waldman, G.D, 1970. A study of drop breakup behind strong shocks with applications to flight, AVCO Report, AVSD-0110-70-77.

Reitz, R.D., Bracco, F.V., 1986. Mechanism of breakup of round liquid jets. In: Encyclopedia of Fluid Mechanics. Gulf Publishing, Houston, TX, p. 223.

Stapper, B.E., Samuelson, G.S., 1990. An experimental study of the breakup of a two dimensional liquid sheet in the presence of co-flow air shear, American Institute of Aeronautics and Astronautics, paper AIAA-90-0461, 28th Aerospace Science Meeting, 8–11 January, Reno, NV.

Wierzba, A., Takayama, K., 1988. Experimental investigation of the aerodynamic breakup of liquid drops. AIAA J. 26, 1329–1335.

Wierzba, A., 1990. Deformation and breakup of liquid drops in a gas stream at nearly critical Weber numbers. Experiments in Fluids 9, 59–64.

Wu, P.K., Faeth, G.M., 1993. Aerodynamic effects primary breakup of turbulent liquids. Atomization and Sprays 3, 265–289.

Wu, P.K., Hsiang, L.P., Faeth, G.M., 1993. Aerodynamic effects on primary and secondary spray breakup. In: First International Symposium on Liquid Rocket Combustion, Pennsylvania State University, University Park, PA.